Original Article

PRSS3 is a potential prognostic biomarker for lung adenocarcinoma

Lu Nie^, Xueqing Zhang, Jie Wu

Department of Oncology, The First Affiliated Hospital of Jinzhou Medical University, Jinzhou, China

Contributions: (I) Conception and design: L Nie; (II) Administrative support: J Wu, X Zhang; (III) Provision of study materials or patients: J Wu; (IV) Collection and assembly of data: L Nie; (V) Data analysis and interpretation: J Wu, L Nie; (VI) Manuscript writing: All authors; (VII) Final approval of manuscript: All authors.

Correspondence to: Jie Wu, MD, PhD. Department of Oncology, The First Affiliated Hospital of Jinzhou Medical University, No. 2, Section 5, Renmin Street, Guta District, Jinzhou 121000, China. Email: Jiewu8058@163.com.

Background: Lung adenocarcinoma (LUAD) is a highly prevalent and deadly form of lung cancer and is a significant health concern worldwide. Although the expression of serine protease 3 (PRSS3) is elevated in certain cancers, its function in LUAD is yet unclear. The aim of this study was to investigate the mechanism of PRSS3 in lung adenocarcinoma, and validate PRSS3 as a reliable prognostic biomarker in lung adenocarcinoma.

Methods: The Cancer Genome Atlas (TCGA) provides RNA expression data and patient medical information for LUAD patients. To determine which genes are expressed differently in LUAD and normal lung tissues, we carefully examined these data. We then used Cox regression analysis to examine the expression and survival data to pinpoint the genes that are strongly associated with patient survival. The PRSS3 gene affects patient prognosis. Afterward, we divided LUAD patients into low- and high-expression groups on the basis of the median PRSS3 expression to examine the relationship between immune cells and PRSS3. The results of the CIBERSORT and CIBERSORTx studies revealed correlations between PRSS3 and the degree of infiltration of several immune cell types. After the groups with low and high PRSS3 expressions were compared, PRSS3-related genes were identified, and functional enrichment analysis was performed. Furthermore, a model was developed to predict patient prognosis according to clinical characteristics and PRSS3 expression. After the bioinformatics analyses were completed, we validated the differential expression of PRSS3 in samples obtained from our center via Western blotting and immunohistochemistry (IHC).

Results: We found that PRSS3 expression is highly upregulated in LUAD and that high PRSS3 expression is associated with a poorer prognosis in the TCGA database. Single-sample gene enrichment analysis revealed a strong correlation between PRSS3 and the immunological microenvironment. The clinical model developed on the basis of the PRSS3 showed great accuracy and can be used as a significant diagnostic indicator for LUAD. Western blotting and IHC confirmed a substantial increase in PRSS3 expression in LUAD. Herein, we analyzed an available dataset for a clinical cohort and revealed that elevated levels of PRSS3 are indicative of unfavorable outcomes in patients diagnosed with LUAD.

Conclusions: PRSS3 is significantly upregulated in LUAD and can be used as a marker for LUAD diagnosis and prognosis assessment. Further study of PRSS3 could provide valuable insight into the mechanisms underlying the occurrence and progression of LUAD.

Keywords: Lung adenocarcinoma (LUAD); prognosis; serine protease 3 (PRSS3); immunohistochemistry (IHC); Western blotting

^ ORCID: 0009-0001-5409-9523.

Submitted Jul 07, 2024. Accepted for publication Nov 10, 2024. Published online Feb 05, 2025.
doi: 10.21037/tcr-24-1556
View this article at: https://dx.doi.org/10.21037/tcr-24-1556

Introduction

As one of the most common malignancies in the world, lung cancer has a significant economic impact on society (1). In recent years, China and other countries have seen a significant increase in the number of lung cancer diagnoses and deaths associated with this disease (2). Lung cancer is the second most common type of cancer, with the American Cancer Society reporting over 2.2 million new cases each year. With approximately 1.8 million deaths from cancer, lung cancer is the disease that causes the greatest number of cancer-related deaths overall (3). Despite improvements in the previous ten years in the detection and treatment of lung cancer, many patients still have a poor prognosis (4), with a 5-year overall survival (OS) rate of only 16% (5). Lung adenocarcinoma (LUAD) is the most common pathological type of lung cancer (6). Hence, identifying viable prognostic biomarkers that can aid in tailoring treatment and significantly improve the prognosis of LUAD patients is imperative. Government-funded cancer genomics databases and repositories, such as The Cancer Genome Atlas (TCGA) (7), offer large functional genomics datasets associated with different types of cancer. These resources enable comprehensive pan-cancer analyses (8).

Proteases are involved in many important biological processes and are linked to a broad range of pathological disorders, including the development of cancer (9). Trypsin belongs to the family of serine proteases, which are essential for many pathological processes, such as the development of cancer (10-13). One of the main types of trypsinogen is PRSS3, which is also called serine protease 3 (14). PRSS3 was first identified in the brain (15). This might be a splice variation of trypsinogen. PRSS3 is synthesized in the pancreas, specifically in acinar cells. In the human body, the primary role of PRSS3 is to facilitate the digestion and absorption of food by acting as an enzymatic and catabolic trypsin inhibitor when it is delivered to the small intestine (16). Moreover, a growing body of evidence suggests a strong relationship between PRSS3 and the evolution and course of multiple cancers, including liver cancer, breast cancer, gastric cancer, colon adenocarcinoma, pancreatic cancer, and epithelial ovarian cancer (17-21). For example, in lung cancer, the study by Zhou *et al.* Revealed the mechanism of action of PRSS3 in circulating lung cancer cells (22). When circulating tumor cells (CTCs) travel in circulation, they can be killed by detachment-induced anoikis and fluidic shear stress (SS)-mediated apoptosis. SS triggers PRSS3 to cleave the N-terminal inhibitory domain of PAR2 within 2 h. As a G protein-coupled receptor, PAR2 further activates the G protein to turn on the Src-ERK/p38/JNK-FRA1/cJUN axis to promote the expression of epithelial-mesenchymal transition markers, and to promote the invasion and metastasis of circulating cancer cells.

Nevertheless, our current knowledge of PRSS3 expression, regulation, and function in LUAD is still limited. We investigated the connection between PRSS3 expression and the tumor immune microenvironment by employing the CIBERSORT method. Furthermore, to reveal the possible biological roles and pathways of PRSS3 in LUAD, Kyoto Encyclopedia of Genes and Genomes (KEGG) and Gene Ontology (GO) enrichment analyses were used. By integrating patient clinical information with PRSS3 expression, we constructed a prediction model that provides a more precise estimation of patients' OS. Finally, we verified the expression of PRSS3 in LUAD by immunohistochemistry (IHC) and western blotting. Overall, these results indicate that PRSS3 might be a prognostic indicator for LUAD. We present this article in

Highlight box

Key findings

- Serine protease 3 (PRSS3) may be a promising prognostic biomarker for lung adenocarcinoma (LUAD).

What is known and what is new?

- It has been reported that PRSS3 is abnormally expressed in multiple tumors and is associated with tumor the evolution and course.
- We investigated the potential functional role of PRSS3 in LUAD using bioinformatics analysis. Moreover, Western blotting and immunohistochemistry (IHC) results showed that LUAD tissues expressed more PRSS3 than did normal tissues.

What is the implication, and what should change now?

- In the future, molecular biology experiments will be conducted to further explore the mechanism of action of PRSS3 in LUAD.

accordance with the TRIPOD reporting checklist (available at https://tcr.amegroups.com/article/view/10.21037/tcr-24-1556/rc).

Methods

Data sources

The TCGA database (https://portal.gdc.cancer.gov/) provides downloadable mRNA expression information, an overview of mutations, and medical information for patients with LUAD. The dataset we assessed comprises transcriptome data for 568 samples (58 normal samples and 510 tumor samples). For this study, Limma, an R package (version 3.54.2), was used to analyze the variations in gene expression between healthy tissues and tumor tissues.

Identification of prognostic genes

We further identified differentially expressed genes (DEGs) associated with OS via univariate Cox regression analysis. In this part of the study, the R packages survival (3.6-4), forestplot (3.1.3), and tidyverse (2.0.0) were used, and a screening threshold with a P value less than 0.0001 was applied. Furthermore, we constructed a forest map.

Analysis of the TIMER database

TIMER (https://cistrome.shinyapps.io/timer/) (23) is a user-friendly web application that was used to analyze the differential expression of specific genes of interest in the TCGA database in tumor tissues versus precancerous tissues.

UALCAN database analysis

An online study of differential gene expression in cancer and normal tissues was performed via the UALCAN database (http://ualcan.path.uab.edu/) (24) using data from the TCGA. The UALCAN database was used to group patients on the basis of gene expression levels and compare the survival of different expression groups.

Assessment of the immune microenvironment

The composition of 22 human immune cells was classified via the LM22 gene signature and the CIBERSORTx algorithm (25). In this part of the study, the parallel (4.4.0) and e1071 (1.7-14) R packages were used. Using the single-sample gene set enrichment analysis (ssGSEA) (26) technique, we calculated the extent of infiltration of 28 different types of immune cells (27). In this part of the study, the gene set variation analysis (GSVA) (1.52.3), data.table (1.15.4), tidyverse (2.0.0), remotes (2.5.0) R packages were used.

Landscape of somatic mutations in LUAD

The tumor mutational burden (TMB) denotes the total number of somatic mutations per megabase (Mut/Mb) of DNA, encompassing deletions, insertions, substitutions, and translocations (28). In this part of the study, the maftools (2.20.0), tidyverse (2.0.0), readxl (1.4.3), and readr (2.1.5) R packages were used.

Functional enrichment analysis

Based on the grouping of median values of PRSS3 expression (0–50% for low expression group and 50-100% for high expression group), we classified LUAD patients into PRSS3 high and low expression groups. The R package "DESeq2" (29) version 1.26.0 was used to identify DEGs between the high-PRSS3 expression group and the low-PRSS3 expression group. The threshold for significance was set as an adjusted P value <0.05 and |log2fold change (FC)| >1. To further investigate the role of PRSS3 in LUAD, the "ClusterProfiler" (30) package in R was used to identify enriched GO functions and KEGG pathways (P<0.05). In addition, the R packages BiocManager (1.30.23) and org.Hs.eg.db (3.19.1) were also used.

Prognostic model construction and evaluation

Nomograms are visual aids that provide risk model results in an understandable and efficient way, making it easier to predict the outcome. Line length in nomogram models indicates how much each variable and various variable values influence the result (31). Univariate and multivariate Cox regression analyses were performed via R software and the "survival" package (32) to evaluate the associations of PRSS3 expression and other clinical factors with LUAD prognosis. To predict the 1-, 3-, and 5-year OS of LUAD patients, a prognostic model was created by combining various clinical prognostic factors. The Nomogram was constructed using the following R packages: rms(6.8-1), regplot(1.1), ggDCA(1.2), ggprism(1.0.5). To assess the

nomogram's performance, a calibration curve was used (33). Prognostic features were then used to create receiver operating characteristic (ROC) curves, and the area under the curve (AUC) (34) was computed to evaluate how well each prognostic feature detected patients with LUAD. The curves were formed using the ROCR (1.0-11) and timeROC (0.4) R packages.

In-house cohort and sample collection

In 2024, 8 pairs of newly excised LUAD tissues and corresponding adjacent normal tissues from the First Affiliated Hospital of Jinzhou Medical University were collected for protein level detection. These tissues were promptly transported and stored in a −80 ℃ refrigerator following surgical removal. Additionally, paraffin sections of LUAD tissues from 99 patients who underwent surgery in 2019 from the Department of Pathology of the First Affiliated Hospital of Jinzhou Medical University were collected for immunohistochemical analyses. The study was conducted in accordance with the Declaration of Helsinki (as revised in 2013). This study was approved by the Institutional Research Ethics Committee of The First Affiliated Hospital of Jinzhou Medical University (No. KYLL-2024339) and informed consent was taken from all the patients.

Main reagents

Tissue protein extraction kit (Beyotime, Shanghai, China), BCA protein concentration assay kit (Beyotime), high-sensitivity ECL chemiluminescence kit (Beyotime), DAB chromogenic kit (Beyotime).

Western blotting

Using a tissue protein extraction kit, the required tissue homogenate was produced. The homogenate was then allowed to lyse on ice and centrifuged for 25 minutes at 4 ℃ at a speed of 13,000 revolutions per minute. After protein quantification via the BCA technique, the desired total protein was found in the resulting supernatant. After the proteins were combined with five volumes of protein buffer, they were heated for fifteen minutes in a metal bath. The final samples were divided into equal portions and stored at −20 ℃ in a refrigerator. Sodium dodecyl sulfate polyacrylamide gel electrophoresis (SDS-PAGE) was used to separate the protein samples. Afterward, the proteins were placed onto polyvinylidene fluoride (PVDF) membranes, which were sealed for an hour in a solution containing 5% milk powder. The primary antibody was then added and incubated overnight at 4 ℃ after being diluted as needed. The antibodies used were in Table S1. Every other day, the membranes were washed three times with TBST. After the membranes were coated with the secondary antibody, they were incubated for an hour at 25 ℃. After three rounds of washing, the PVDF membranes were analyzed by autoradiography to identify the protein bands. The sample was finally detected via an enhanced chemiluminescence (ECL) device.

IHC

The process of IHC staining was executed after xylene deparaffinization and progressive rehydration with ethanol. After 30 minutes of boiling in citrate-EDTA antigen retrieval solution, the tissue slices were allowed to cool to room temperature. Afterward, a 3% H_2O_2 solution was used to block the inherent peroxidase activity. The sections were then treated with primary antibodies and left in an incubator overnight at 4 ℃. After multiple thorough washes, the sections were incubated for 40 minutes at room temperature with the secondary antibody. Hematoxylin was used to restrict the sections after they had been chromatographed via the DAB Horseradish Peroxidase Color Development Kit. After neutral balsam was applied to the slides, a microscope was used to view and take pictures of the slides.

Statistical analysis

We conducted the statistical analyses and generated graphs via R software (version 4.4.0), GraphPad Prism software (version 8.0.2), SPSS (version 26.0), and ImageJ. Wilcoxon test was employed for comparing gene expression differences between normal and tumor tissues. Kaplan-Meier survival analysis and the Log rank test were used to plot the survival curve and compare the survival time, test level α=0.05. The comparison between the means of two independent samples was performed using the *t*-test. To evaluate the correlation between PRSS3 expression and the other variables, we performed Spearman correlation test and Kruskal-Wallis test. We stratified the cohort into patients with a high or low median PRSS3 expression median as the cut-off value. Univariate Cox regression and Multivariate Cox regression analysis was conducted to identify

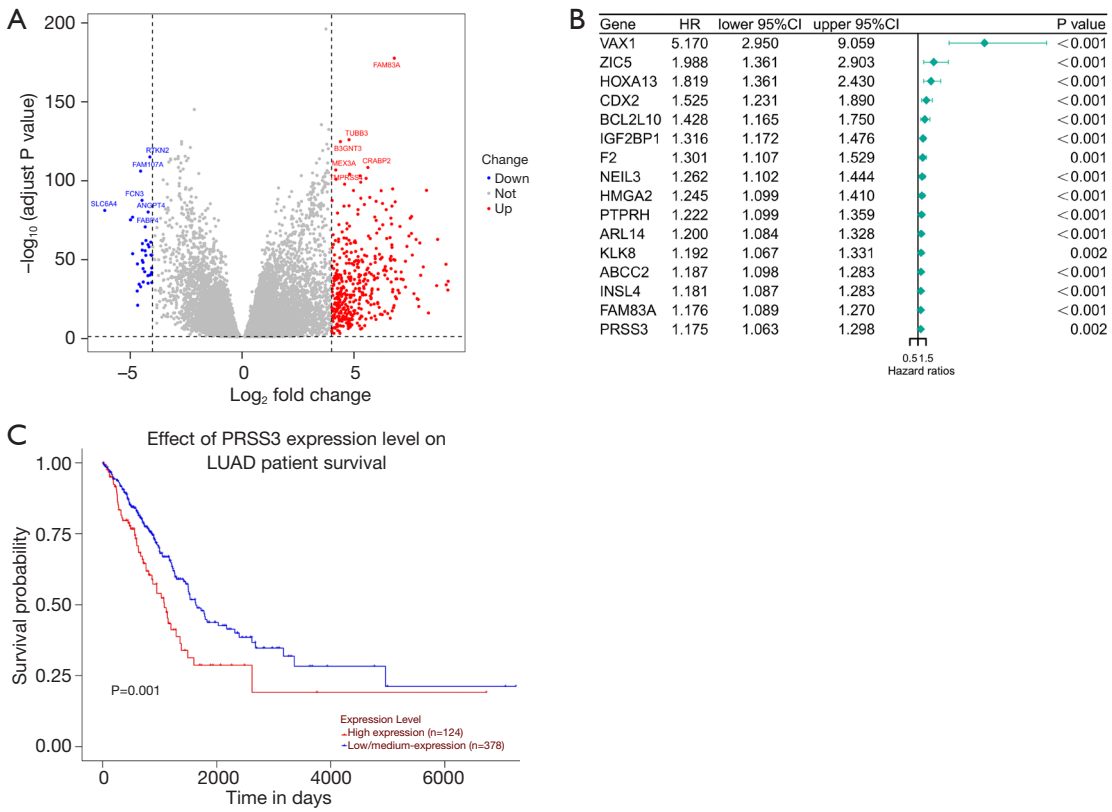

Figure 1 Identification of differentially expressed genes. (A) Volcano plot demonstrating the DEGs. (B) Forest map of DEGs related to LUAD patient survival analyzed by univariate Cox regression. (C) Survival curves of LUAD patients with different PRSS3 expression levels. LUAD, lung adenocarcinoma; DEGs, differentially expressed genes; PRSS3, serine protease 3; HR, hazard ratio; CI, confidence interval.

independent prognostic factors. A significance level of 0.05 was employed as the threshold for statistical significance in all studies. To ensure validity, the experiments were replicated three times.

Results

Identification of prognosis-related DEGs in LUAD

After careful screening, we selected 510 cancer samples and 58 normal samples for analysis. A total of 441 DEGs were identified ($|\log_2 FC| > 4$, P adj<0.05), including 405 upregulated and 36 downregulated genes (*Figure 1A*). Afterward, the patients' survival information was fitted to the expression data for the highly expressed genes, and univariate Cox regression analyses were performed. The 16 genes with the highest correlation with poor patient prognosis were identified by screening, with P<0.05 and HR >1 as the thresholds (*Figure 1B*). PRSS3 is among the top 16 prognostic genes. According to the literature, the mechanism of action of PRSS3 in LUAD is still unclear. We utilized the UALCAN database to assess the prognostic value of PRSS3 in LUAD by generating Kaplan-Meier survival curves for patients grouped according to the PRSS3 expression level (*Figure 1C*). Patients with elevated levels of PRSS3 had considerably poorer OS than those with lower PRSS3 levels did (P<0.005).

PRSS3 overexpression in LUAD

According to the TIMER database, numerous tumor types, particularly LUAD, exhibit significantly elevated PRSS3 expression (*Figure 2A*). We next assessed PRSS3 expression in LUAD through the UALCAN database (*Figure 2B*). We analyzed the downloaded LUAD data with the R package tidyverse (version 2.0.0). Compared with those in tumor samples, PRSS3 expression levels were lower in normal samples (*Figure 2C*).

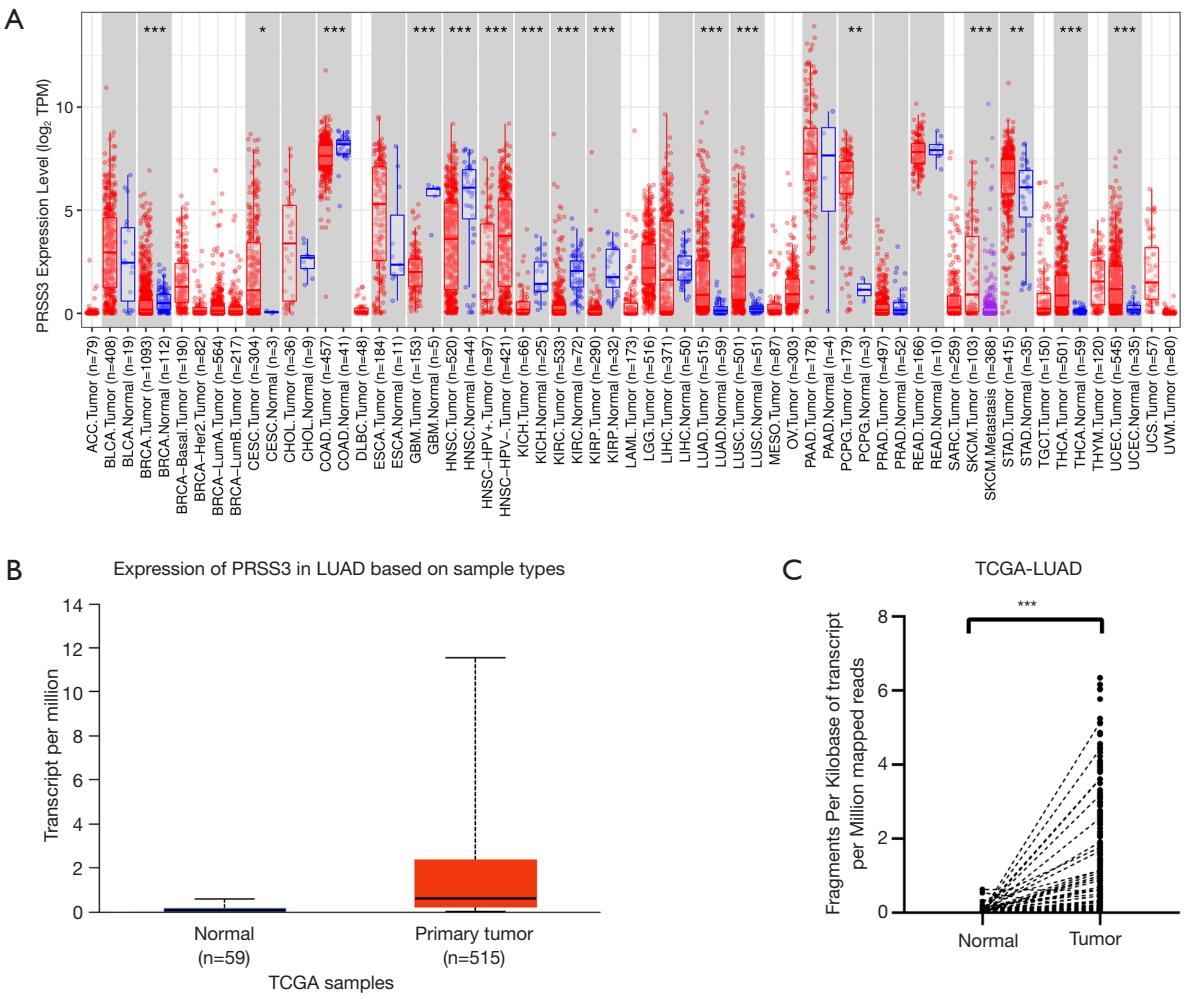

Figure 2 Analysis of PRSS3 expression in multiple databases. (A) Expression levels of PRSS3 in different cancer types according to TIMER. (B) Box plot comparing PRSS3 expression in LUAD derived from UALCAN (TPM). (C) Analysis of the expression levels of PRSS3 in both normal and tumor tissues in the TCGA-LUAD dataset (FPKM). ***, P<0.001; **, P<0.01; *, P<0.05. PRSS3, serine protease 3; LUAD, lung adenocarcinoma; TCGA, The Cancer Genome Atlas; TPM, transcripts per million; FPKM, fragments per kilobase of transcript per million fragments mapped.

PRSS3 expression and the immune microenvironment of LUAD

To evaluate the relationships between PRSS3 expression and the degree of immune cell infiltration, correlation analyses were performed. Using CIBERSORT locally, the abundance ratio matrix of 22 distinct tumor-infiltrating cell types was computed for 510 samples (*Figure 3A*). Furthermore, LUAD patients were categorized into groups according to the median PRSS3 level, which separated patients with high and low PRSS3 expression levels. Using CIBERSORTx analysis, we compared the characteristics of the tumor immune microenvironment between the groups with high and low PRSS3 expression. A positive correlation (P<0.05) was found between the frequencies of activated memory CD4 T cells, M0 macrophages, and active mast cells and PRSS3 expression, according to the results of CIBERSORTx analysis. On the other hand, PRSS3 expression was negatively correlated (P<0.05) with the percentages of resting memory $CD4^+$ T cells, naive B cells, $CD8^+$ T cells, and resting mast cells (*Figure 3B*). Additionally, PRSS3 expression and the proportions of several immune cell types, such as activated CD4 T cells, effector memory CD4 T cells, gamma

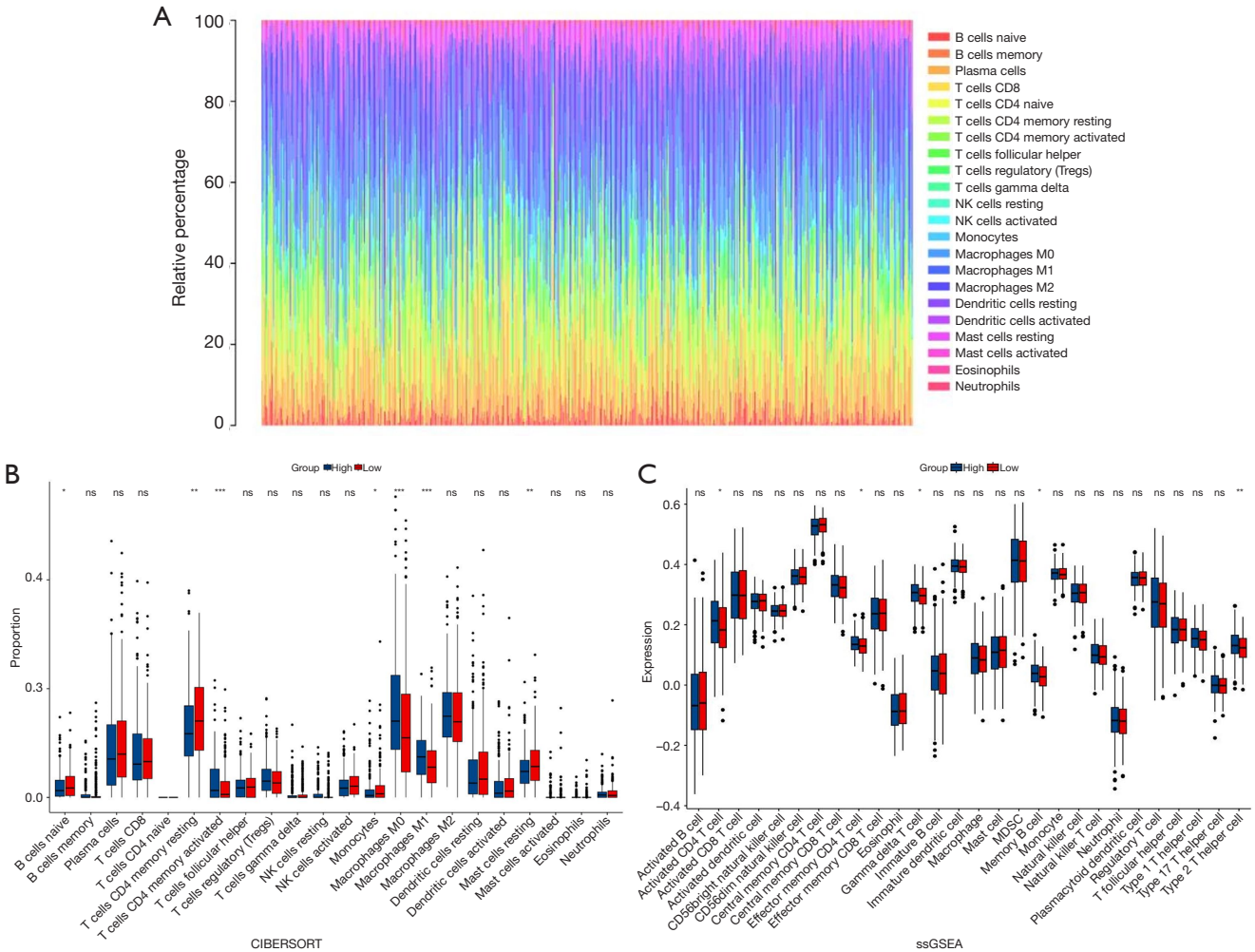

Figure 3 Integrative analysis of PRSS3 expression in TIICs. (A) Overview of tumor-infiltrating immune cells. (B) Proportions of 22 tumor-infiltrating immune cell types between LUAD patients in the high PRSS3 expression group and those in the low PRSS3 expression group. (C) ssGSEA of the low- and high-PRSS3 expression groups. ns, not significant; *, P<0.05; **, P<0.01; ***, P<0.001. PRSS3, serine protease 3; TIICs, tumor-infiltrating immune cells; LUAD, lung adenocarcinoma; ssGSEA, single-sample gene set enrichment analysis; NK, natural killer; MDSC, myeloid-derived suppressor cell.

delta T cells, memory B cells, and type 2 T helper cells, were positively correlated (P<0.05) according to ssGSEA (*Figure 3C*).

Exploring the somatic mutations in LUAD

We obtained the somatic mutation profiles of 616 LUAD patients from the TCGA database. The mutation landscape was displayed via the "maftools" R package. Different mutation types are represented in various colors with annotations at the bottom. The top 10 genes with the highest mutation frequency were TP53 (50%), TTN (43%), MUC16 (41%), CSMD3 (39%), RYR2 (34%), LRP1B (32%), ZFHX4 (31%), USH2A (29%), KRAS (26%), and FLG (23%) (*Figure 4A*).

In addition, missense mutations are the most common type of mutation, while single nucleotide polymorphisms (SNPs) constitute a greater proportion of mutations than insertions or deletions. The predominant single nucleotide variant (SNV) observed in LUAD samples was the change

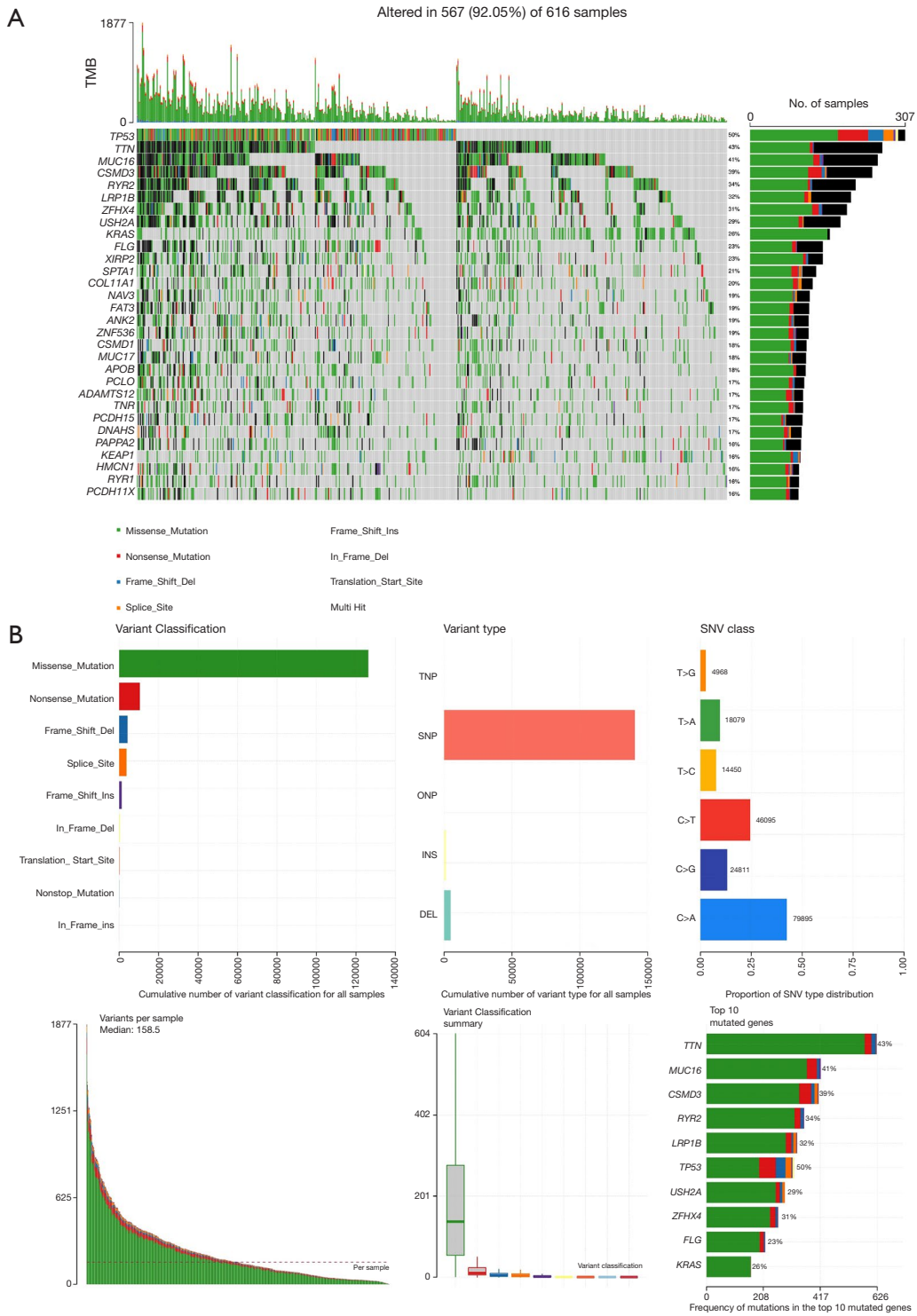

Figure 4 Exploring the mutation profiles in LUAD samples. (A) The mutation frequency is displayed in the left panel, with genes arranged according to their respective mutation frequencies. The lower panel displays various types of mutations. (B) Classification of variations, types, and categories of single nucleotide variants in LUAD samples. LUAD, lung adenocarcinoma; TMB, tumor mutational burden; TNP, triple nucleotide polymorphism; SNP, single nucleotide polymorphism; ONP, oligonucleotide polymorphism; INS, insertion; DEL, deletion; SNV, single nucleotide variation.

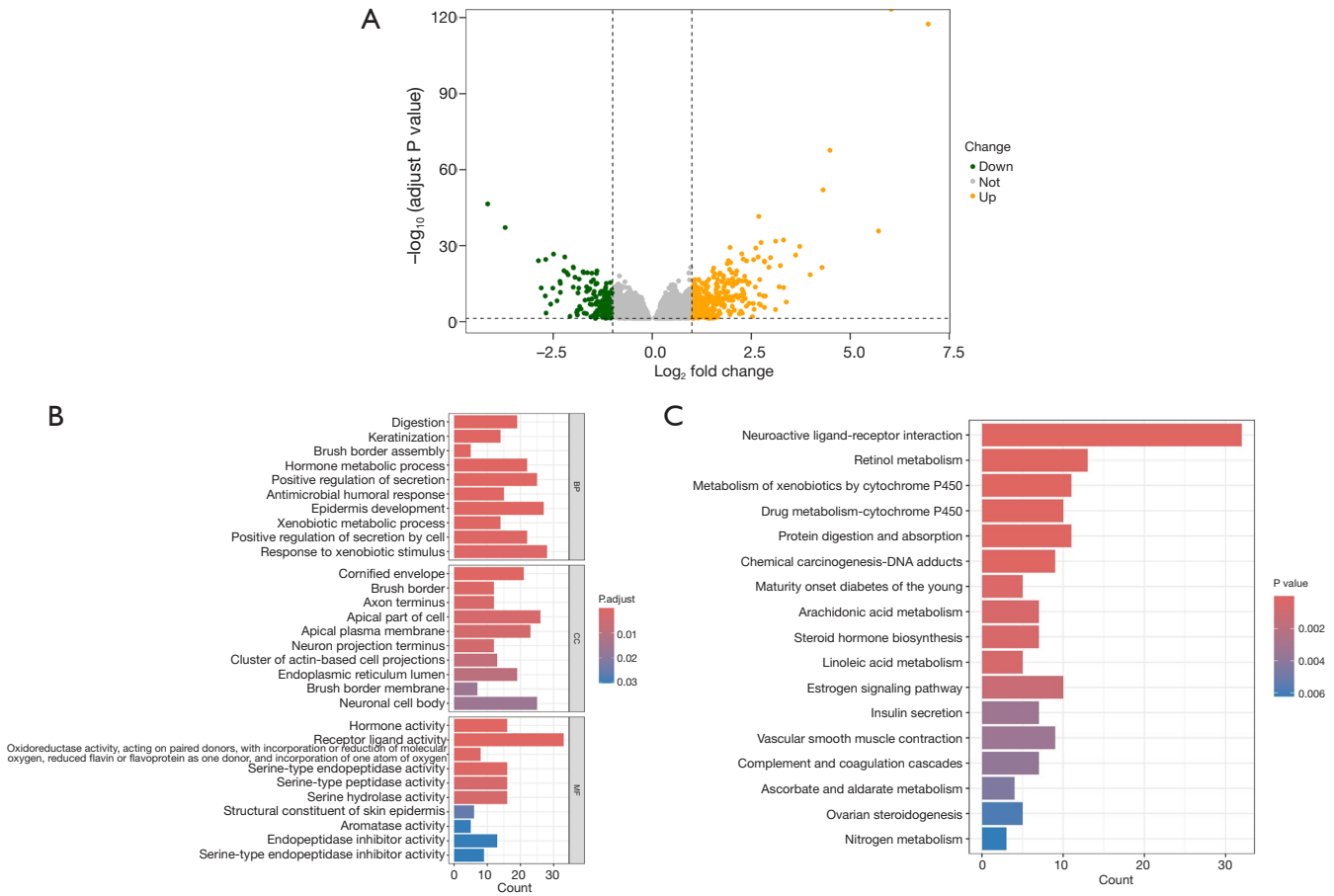

Figure 5 Results of the functional enrichment analysis of DEGs related to PRSS3. (A) Volcano plots were drawn to show the DEGs between the high and low PRSS3 expression groups. (B) GO enrichment analysis of the DEGs. (C) KEGG enrichment analysis of the DEGs. PRSS3, serine protease 3; DEGs, differentially expressed genes; GO, Gene Ontology; KEGG, Kyoto Encyclopedia of Genes and Genomes; BP, biological process; CC, cellular component; MF, molecular function.

from C to A (*Figure 4A*). Moreover, the number of variations in each sample was computed, and the frequencies of different types of mutations are presented in a box plot; the different colors indicate different mutation types, and the data are shown for LUAD samples (*Figure 4B*).

In contrast, the mutation frequency of PRSS3 is 0%. These data indicate that PRSS3 does not affect the prognosis of LUAD patients by affecting their TMB.

Functional enrichment analysis of DEGs related to PRSS3

In this study, we assessed the potential role of PRSS3 in LUAD via differential expression analysis. We divided patients with LUAD into high and low PRSS3 expression groups (on the basis of the median PRSS3 expression value) for comparison, and each group included 255 LUAD patients. The R package "DESeq2" was subsequently used to screen for DEGs associated with PRSS3. A total of 527 genes were found to be differentially expressed, with 353 genes being upregulated and 174 genes being downregulated. The results are shown via volcano maps; the threshold criteria were a $|\log FC| > 1.0$ and $P<0.05$ (*Figure 5A*). The mRNA expression profiles of these genes varied significantly between the high- and low-PRSS3 subgroups.

GO and KEGG enrichment analysis indicated that DEGs associated with PRSS3 are involved in several biological process (BPs), including digestion, positive regulation of secretion, hormone metabolic processes, brush boundary assembly, and keratinization. In addition, it is also implicated in cellular component (CC) and molecular function (MF). The CCs included the neuronal cell body,

brush border membrane, endoplasmic reticulum lumen, cluster of actin-based cell projections, neuron projection terminus, and apical plasma membrane. The MFs included serine hydrolase activity, serine-type peptidase activity, serine-type endopeptidase activity, receptor-ligand activity, and hormone activity (*Figure 5B*).

In addition, KEGG analysis (*Figure 5C*) revealed the involvement of PRSS3 in various pathways, such as neuroactive ligand-receptor activation, insulin secretion, the estrogen signaling pathway, arachidonic acid metabolism, drug metabolism—cytochrome P450, metabolism of xenobiotics by cytochrome P450, and retinol metabolism.

Development of a nomogram combining the PRSS3 score and clinical variables for LUAD

To create a predictive model for OS in patients with LUAD, univariate Cox analysis of various clinical factors was first performed, and it was found that tumor stage, T stage, N stage, and PRSS3 expression significantly affected the prognosis of patients with LUAD (*Figure 6A*). A multivariate Cox analysis was subsequently performed for several of the above factors (*Figure 6B*). By utilizing the above results, a predictive model was developed, and a visually appealing nomogram was created to predict the 1-, 3-, and 5-year OS probabilities for each patient with LUAD (*Figure 6C*). Moreover, calibration curves were constructed to assess the accuracy of the nomograms (*Figure 6D*). The calibration analysis revealed a strong fit between the calibration line and the ideal curve, suggesting a significant correlation between the predicted and observed values. These findings indicate a close association between predictive factors and OS in patients with LUAD. The specificity and sensitivity of the prognostic model were evaluated via time-dependent ROC curves (*Figure 6E*).

Expression of PRSS3 protein in LUAD and adjacent lung tissues

To confirm the significance of PRSS3 in the development and progression of LUAD, we first analyzed the status of PRSS3 expression in LUAD tissue samples. The protein expression levels of PRSS3 were assessed in 8 sets of tumor tissues and their corresponding neighboring noncancerous tissues (*Figure 7A*). The protein expression level of PRSS3 was significantly greater in the tissue samples of patients with LUAD (*Figure 7B*). Further evidence for the role of PRSS3 in LUAD was obtained via immunohistochemical analyses of postoperative pathological sections from patients with LUAD. Protein expression status was assessed by IHC. The immunohistochemical results revealed PRSS3 expression in normal tissues adjacent to LUAD tissues (*Figure 8A*). In tumor tissues, positive immunohistochemical staining for PRSS3 was primarily observed in the extracellular region or secreted region (*Figure 8B-8D*). A total of 99 tissue samples were analyzed for PRSS3 expression. Among these samples, 60 had positive PRSS3 staining, resulting in a positivity rate of 60.6% (60/99), indicating that patients predominantly displayed moderate to strong positivity. These 35 patients were categorized into the high-PRSS3 group.

Relationships between clinicopathological characteristics and PRSS3 expression in our patient cohort with LUAD

The baseline data of our cohort consisting of participants with LUAD were summarized, revealing a link between PRSS3 expression and patient clinical features (*Table 1*). The findings revealed a strong correlation between increased levels of PRSS3 and the progression of lymph node metastasis (P=0.007) and tumor stage (P=0.009). There was no notable link between the expression of PRSS3 and other clinicopathological features (P>0.05).

OS of LUAD patients with different PRSS3 expression patterns

Our findings demonstrated a strong relationship between PRSS3 expression and the prognosis of LUAD patients. Different levels of PRSS3 expression were used to produce Kaplan-Meier survival curves (*Figure 9*). There were 36 patients with low PRSS3 expression and 60 patients with high PRSS3 expression. Kaplan-Meier curve comparison revealed that patients with low PRSS3 expression had much higher OS rates than those with high PRSS3 expression. These findings support the significant role that PRSS3 plays in LUAD and suggest that PRSS3 may be a predictive biomarker for this condition.

Discussion

Lung cancer is a widespread and serious form of cancer that poses a significant threat to human health on a global scale (35). It has a high incidence and death rate, surpassing breast, brain, colorectal, and prostate cancers combined. Among them, LUAD is the most common pathological

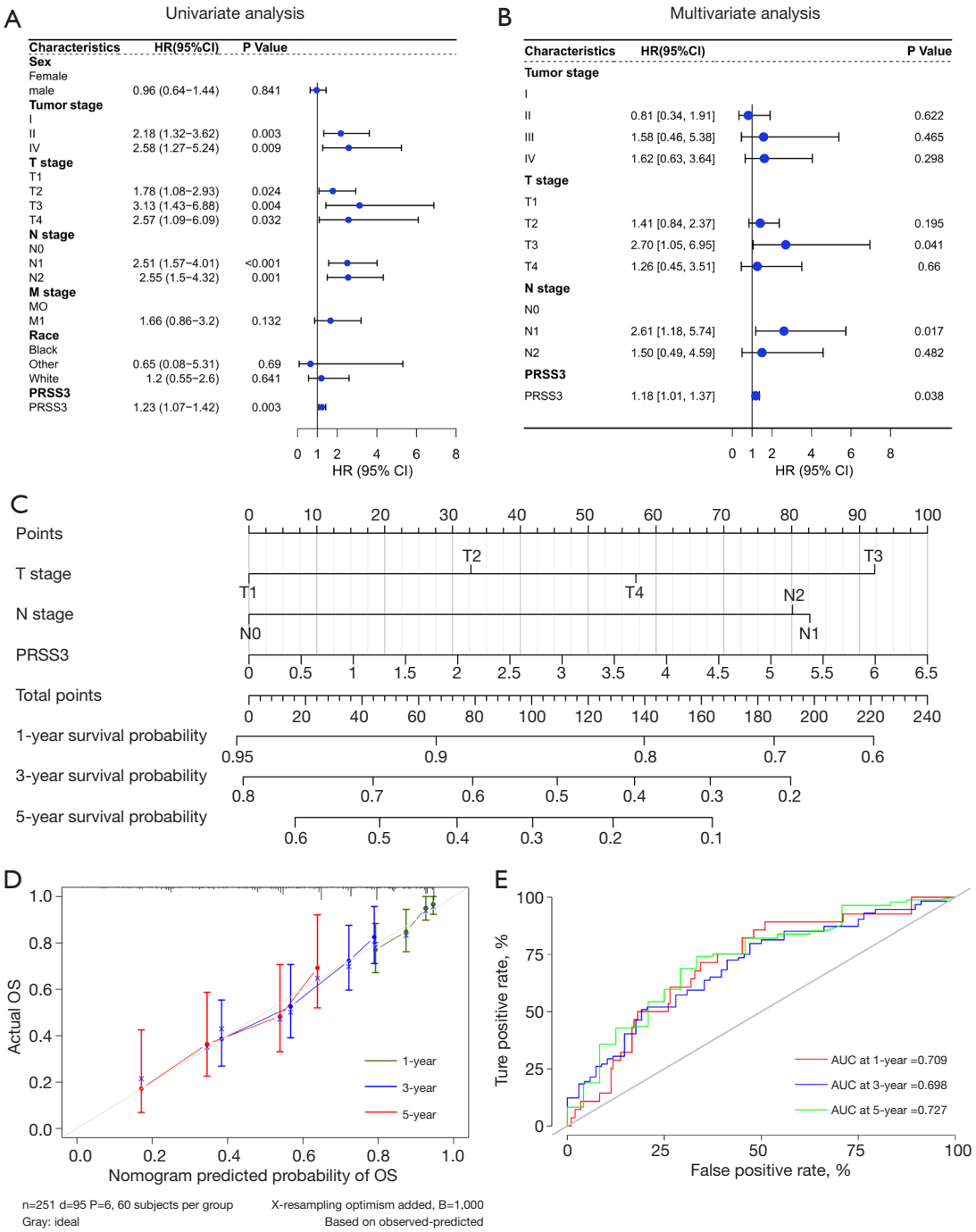

Figure 6 Prognostic significance of PRSS3 in LUAD. (A) Univariate Cox regression analyses revealed that clinical features were significantly related to prognosis. (B) Multivariate Cox regression analysis verified the independent prognostic value of PRSS3. (C) To predict OS with this nomogram, a value needs to be assigned to each factor by drawing a line upward to the benchmark line, summing the points, and extending a vertical line from the total points line to ascertain the projected likelihood of patient survival. (D) The likelihood of survival at 1, 3, and 5 years was evaluated via nomogram calibration plots. The x-axis indicates the predicted survival from the nomogram, whereas the y-axis denotes the observed survival rates. (E) ROC curves for nomograms based on clinical variables and PRSS3 for predicting survival at certain times in the TCGA cohort. PRSS3, serine protease 3; HR, hazard ratio; CI, confidence interval; OS, overall survival; AUC, area under the curve; LUAD, lung adenocarcinoma; ROC, receiver operating characteristic; TCGA, The Cancer Genome Atlas.

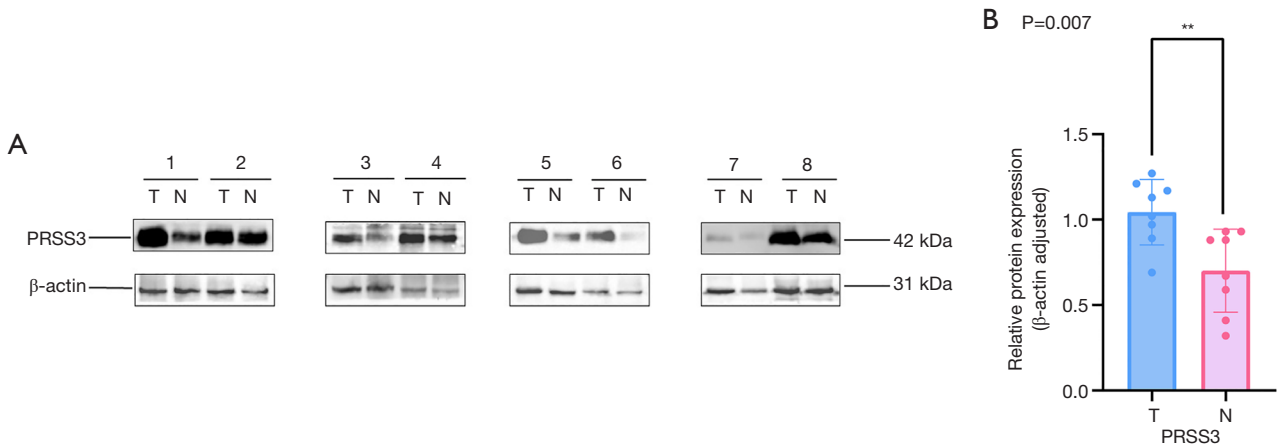

Figure 7 Upregulation of PRSS3 in LUAD tissues. (A) Analysis and comparison of PRSS3 protein expression in 8 LUAD tissues and their corresponding nontumor lung tissues were conducted via Western blotting. β-actin served as the internal reference for this study. (B) Statistical graph showing the protein expression of PRSS3 in 8 pairs of LUAD tissue (T) samples and normal tissue (N) samples. **, P<0.01. PRSS3, serine protease 3; LUAD, lung adenocarcinoma.

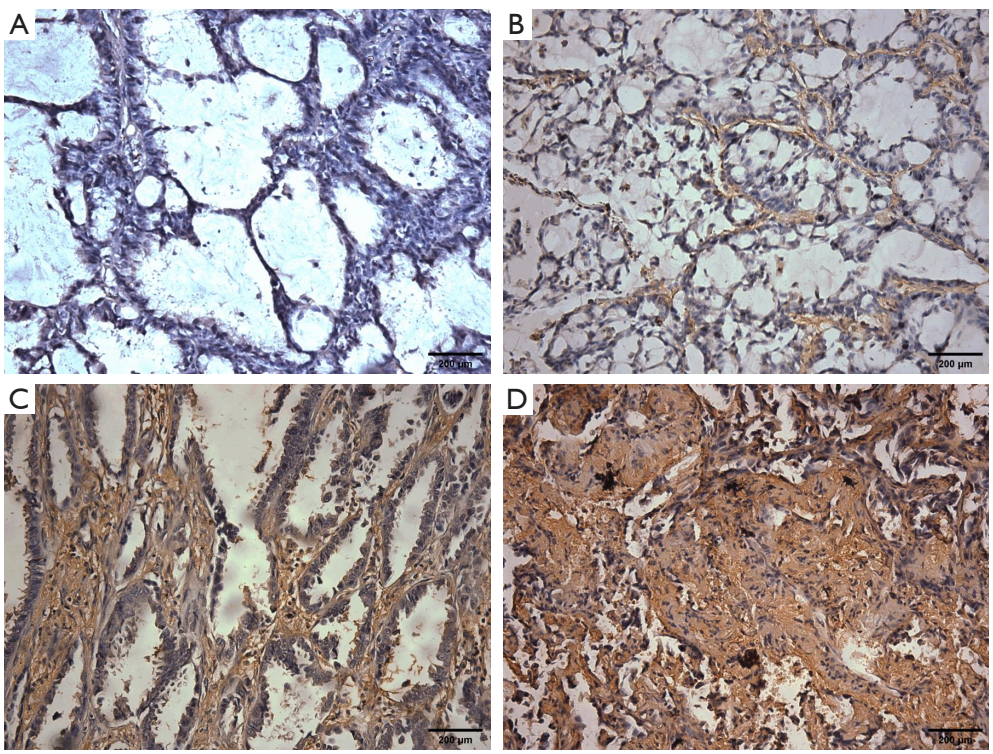

Figure 8 IHC analysis of PRSS3 in LUAD tissues. (A) PRSS3 expression is negative in healthy tissues. (B-D) On the basis of the results of the IHC analysis, three distinct staining levels were identified in the tumor tissues on the basis of the expression level of PRSS3: weak, moderate, and strong. Magnification 200×. PRSS3, serine protease 3; LUAD, lung adenocarcinoma; IHC, immunohistochemistry.

Table 1 Relationships between PRSS3 expression and clinical characteristics in our LUAD cohort

Characteristic	n	PRSS3 high expression, n (%)	PRSS3 low expression, n (%)	χ^2	P value
Age (years)				<0.0001	>0.99
<60	46	28 (46.67)	18 (46.15)		
≥60	53	32 (53.33)	21 (53.85)		
Sex				0.5426	0.46
Male	35	19 (31.67)	16 (41.03)		
Female	64	41 (68.33)	23 (58.97)		
Depth of invasion				0.6693	0.41
T1/T2	96	57 (95.00)	39 (100.00)		
T3/T4	3	3 (5.00)	0 (0)		
Lymph node metastasis				7.3349	0.007
N0	76	40 (66.67)	36 (92.31)		
N+	23	20 (33.33)	3 (7.69)		
Tumor stage				9.4478	0.009
I	76	40 (66.67)	36 (92.31)		
II	15	14 (23.33)	1 (2.56)		
III	8	6 (10.00)	2 (5.13)		
Differentiation				1.1491	0.28
Low differentiation	22	16 (26.67)	6 (15.38)		
Moderate and high differentiation	77	44 (73.33)	33 (84.62)		
Smoking history				0.6113	0.43
No	74	47 (78.33)	27 (69.23)		
Yes	25	13 (21.67)	12 (30.77)		

LUAD, lung adenocarcinoma; PRSS3, serine protease 3.

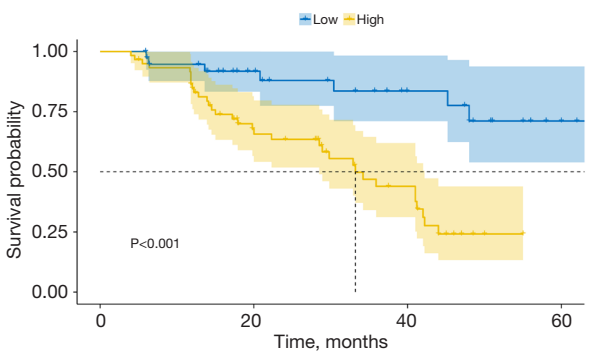

Figure 9 OS differences between the groups with high and low PRSS3 expression. OS, overall survival; PRSS3, serine protease 3.

type of lung cancer (36). Unfortunately, most individuals with LUAD are already in an intermediate to advanced stage at diagnosis (37), further worsening their prognosis. Therefore, investigations of new and effective indicators for the early detection and management of LUAD are crucial. PRSS3 is such a prognostic marker for LUAD.

PRSS3 is a serine protease. Serine proteases can be found in two different forms: either bound to the cell membrane or secreted into the extracellular space. These proteases have crucial functions in immune responses, such as releasing cytokines and activating signaling receptors (38). Dysfunction of serine proteases has been shown to play a

significant role in the development of malignant tumors (12,39).

PRSS3 is also one of the main types of trypsinogen. Moreover, trypsinogen that is produced by three different trypsinogen genes: PRSS1, PRSS2, and PRSS3 (40,41). These genes encode Trypsinogen I, Trypsinogen II, and Trypsinogen IV (also known as intermediate trypsinogen) (18,42). PRSS3 has a relatively small effect on pancreatic exocrine secretion, contributing to only 3–10% of trypsin activity in human pancreatic fluid, unlike PRSS1 and PRSS2 (21).

A thorough bioinformatics analysis was conducted using gene transcript profiles of LUAD samples retrieved from the TCGA database. There were 441 DEGs found between the tumor tissue and normal tissue. Among these genes, 36 genes were upregulated, and 405 genes were downregulated.

To screen for genes related to patient prognosis, we fitted the patient expression data with survival information and screened correlated factors through Cox regression analysis. We identified PRSS3 as a prognostic gene.

Afterward, a thorough examination of the expression of PRSS3 was conducted across various pancancer datasets. Most malignant tumors were found to have higher levels of PRSS3 than normal tissues were, according to the comparison of cancer and normal tissues. Initially, we discovered a significant correlation between the expression levels of PRSS3 and various immune cell types. Through CIBERSORTx analysis, we made interesting observations. There may be a positive correlation between the expression of PRSS3 and certain cell types, namely, CD4 memory-activated T cells, M0 macrophages, and activated mast cells. In contrast, naive B cells, CD8 T cells, resting memory CD4 T cells, and resting mast cells were negatively correlated. These findings suggest that PRSS3 may influence LUAD progression through interactions with specific immune cell populations, potentially affecting immune surveillance and response mechanisms.

Furthermore, ssGSEA supported these observations, as the analysis revealed additional immune cell types positively linked to PRSS3 expression, such as activated $CD4^+$ T cells, effector memory $CD4^+$ T cells, gamma delta T cells, memory B cells, and type 2 T helper cells. These findings emphasize the potential of PRSS3 as an immune response modulator in LUAD and expand our understanding of its involvement in the formation of the tumor immune microenvironment.

Analysis of somatic mutation profiles from TCGA data revealed that PRSS3 itself did not harbor significant mutations across LUAD samples. These findings suggest that PRSS3 may influence LUAD progression through mechanisms independent of mutational events or the TMB.

Differential gene expression analyses of patients in the PRSS3 high-expression and PRSS3 low-expression groups revealed 527 significant changes in gene expression, highlighting potential downstream targets and pathways influenced by PRSS3 in LUAD. Functional enrichment analysis via GO and KEGG pathway analyses revealed the involvement of processes such as digestion, hormone metabolism, and other pathways that are essential for the initiation and spread of cancer.

Univariate and multivariate Cox regression analyses incorporating the PRSS3 signature alongside clinical factors revealed its independent prognostic value. On the basis of these requirements, we developed predictive models for LUAD patient survival. For patients, we created nomograms that showed the likelihood of survival at 1, 3, and 5 years.

The above conclusions are all based on the analysis of the TCGA database. Western blotting and immunohistochemical analysis verified that PRSS3 protein expression was elevated in LUAD tissues compared with adjacent noncancerous tissues. We also investigated the prognostic implications of PRSS3 in LUAD. Survival analysis revealed that patients with high levels of PRSS3 expression had notably worse OS rates than those with lower PRSS3 expression. These findings suggest that PRSS3 may be a useful prognostic indicator for individuals with LUAD, offering insights into its clinical significance and potential as a therapeutic target.

Despite the comprehensive nature of our study, recognizing certain limitations is essential. First, nearly all the data were sourced from public databases, which may lack adequate controls regarding patient age, sex, and other variables that could influence the results. We have only briefly described the immune microenvironment, and have not further explored the mechanism by which PRSS3 affects the immune microenvironment and its impact on the occurrence and development of cancer. More importantly, in cutting-edge research, PRSS3 was found to have different isoforms, which were not further explored in our study. In addition, our analyses relied on a single dataset, which may limit the credibility of our findings across populations and clinical settings. Furthermore, TCGA data on LUAD are limited and insufficient, which may affect the predictive accuracy of this nomogram. Even though we performed both IHC and Western blotting experiments, the sample size remains small.

The functional significance of PRSS3 in LUAD and its molecular mechanisms within the tumor microenvironment have not been validated *in vivo*. More relevant research

or evidence is needed to support the therapeutic efficacy of PRSS3 as a treatment target. In addition, the signaling pathways involved in LUAD development and progression, along with their upstream and downstream molecules, need to be better characterized. Future studies on PRSS3 will aim to address these issues and further investigate the biological role of PRSS3 in LUAD in greater detail, thereby increasing the precision of this study.

Conclusions

This work offers the first thorough examination of PRSS3 in LUAD. Research has revealed that the expression of PRSS3 is greater in tumor tissues than in nearby normal tissues. This study revealed a strong correlation between poor prognosis in LUAD patients and elevated expression of PRSS3. Furthermore, the predictive model we created had better diagnostic accuracy. Finally, our bioinformatics investigation revealed that PRSS3 is a useful biological prognostic marker. These findings lay a solid foundation for future research efforts and offer insightful information for better understanding tumor prevention and treatment.

Acknowledgments

The authors would like to thank the Immunology Laboratory, School of Basic Medical Sciences, Jinzhou Medical University for providing the experimental platform for immunohistochemistry and Western blotting.

Footnote

Reporting Checklist: The authors have completed the TRIPOD reporting checklist. Available at https://tcr.amegroups.com/article/view/10.21037/tcr-24-1556/rc

Data Sharing Statement: Available at https://tcr.amegroups.com/article/view/10.21037/tcr-24-1556/dss

Peer Review File: Available at https://tcr.amegroups.com/article/view/10.21037/tcr-24-1556/prf

Funding: This study was supported by Basic Research General Project of Liaoning Provincial Department of Education (No. LJ212410160079), and the Liaoning Provincial Science and Technology Project Joint Fund Project General Funding Plan (No. 2023-MSLH-048).

Conflicts of Interest: All authors have completed the ICMJE uniform disclosure form (available at https://tcr.amegroups.com/article/view/10.21037/tcr-24-1556/coif). The authors have no conflicts of interest to declare.

Ethical Statement: The authors are accountable for all aspects of the work in ensuring that questions related to the accuracy or integrity of any part of the work are appropriately investigated and resolved. The study was conducted in accordance with the Declaration of Helsinki (as revised in 2013). This study was approved by the Institutional Research Ethics Committee of The First Affiliated Hospital of Jinzhou Medical University (No. KYLL-2024339) and informed consent was taken from all the patients.

References

1. Bade BC, Dela Cruz CS. Lung Cancer 2020: Epidemiology, Etiology, and Prevention. Clin Chest Med 2020;41:1-24.
2. Cao M, Chen W. Epidemiology of lung cancer in China. Thorac Cancer 2019;10:3-7.
3. Siegel RL, Miller KD, Jemal A. Cancer statistics, 2020. CA Cancer J Clin 2020;70:7-30.
4. Ferlay J, Colombet M, Soerjomataram I, et al. Cancer incidence and mortality patterns in Europe: Estimates for 40 countries and 25 major cancers in 2018. Eur J Cancer 2018;103:356-87.
5. Miller KD, Siegel RL, Lin CC, et al. Cancer treatment and survivorship statistics, 2016. CA Cancer J Clin 2016;66:271-89.
6. Deng Z, Cui L, Li P, et al. Genomic comparison between cerebrospinal fluid and primary tumor revealed the genetic events associated with brain metastasis in lung adenocarcinoma. Cell Death Dis 2021;12:935.
7. Shen X, Yan Z, Huang Y, et al. ALDH2 as an

immunological and prognostic biomarker: Insights from pan-cancer analysis. Medicine (Baltimore) 2024;103:e37820.
8. Zhang X, Lai H, Zhang F, et al. Visualization and Analysis in the Field of Pan-Cancer Studies and Its Application in Breast Cancer Treatment. Front Med (Lausanne) 2021;8:635035.
9. Elamin T, Brandstetter H, Dall E. Legumain Activity Is Controlled by Extended Active Site Residues and Substrate Conformation. Int J Mol Sci 2022;23:12548.
10. Jablaoui A, Kriaa A, Mkaouar H, et al. Fecal Serine Protease Profiling in Inflammatory Bowel Diseases. Front Cell Infect Microbiol 2020;10:21.
11. Chen M, Liu X, Hu B, et al. Rabbit Hemorrhagic Disease Virus Non-structural Protein 6 Induces Apoptosis in Rabbit Kidney Cells. Front Microbiol 2019;9:3308.
12. Yang RH, Liang B, Li JH, et al. Identification of a novel tumour microenvironment-based prognostic biomarker in skin cutaneous melanoma. J Cell Mol Med 2021;25:10990-1001.
13. Ferguson TEG, Reihill JA, Martin SL, et al. Novel inhibitors and activity-based probes targeting serine proteases. Front Chem 2022;10:1006618.
14. Yao X, Hu W, Zhang J, et al. Application of cAMP-dependent catalytic subunit β (PRKACB) Low Expression in Predicting Worse Overall Survival: A Potential Therapeutic Target for Colorectal Carcinoma. J Cancer 2020;11:4841-50.
15. Ma R, Ye X, Cheng H, et al. PRSS3 expression is associated with tumor progression and poor prognosis in epithelial ovarian cancer. Gynecol Oncol 2015;137:546-52.
16. Lin S, Xu H, Pang M, et al. CpG Site-Specific Methylation-Modulated Divergent Expression of PRSS3 Transcript Variants Facilitates Nongenetic Intratumor Heterogeneity in Human Hepatocellular Carcinoma. Front Oncol 2022;12:831268.
17. Jiang G, Cao F, Ren G, et al. PRSS3 promotes tumour growth and metastasis of human pancreatic cancer. Gut 2010;59:1535-44.
18. Lin B, Zhou X, Lin S, et al. Epigenetic silencing of PRSS3 provides growth and metastasis advantage for human hepatocellular carcinoma. J Mol Med (Berl) 2017;95:1237-49.
19. Zhang Q, Wang J, Huang D, et al. High Expression of PRSS3 Indicates Unfavorable Clinical Outcomes in Colon Adenocarcinoma. Appl Immunohistochem Mol Morphol 2021;29:564-9.
20. Qian L, Gao X, Huang H, et al. PRSS3 is a prognostic marker in invasive ductal carcinoma of the breast. Oncotarget 2017;8:21444-53.
21. Wang F, Hu YL, Feng Y, et al. High-level expression of PRSS3 correlates with metastasis and poor prognosis in patients with gastric cancer. J Surg Oncol 2019;119:1108-21.
22. Zhou M, Li K, Luo KQ. Shear Stress Drives the Cleavage Activation of Protease-Activated Receptor 2 by PRSS3/Mesotrypsin to Promote Invasion and Metastasis of Circulating Lung Cancer Cells. Adv Sci (Weinh) 2023;10:e2301059.
23. Zhao C, Liu J, Zhou H, et al. NEIL3 may act as a potential prognostic biomarker for lung adenocarcinoma. Cancer Cell Int 2021;21:228.
24. He X, Wang J, Yu H, et al. Clinical significance for diagnosis and prognosis of POP1 and its potential role in breast cancer: a comprehensive analysis based on multiple databases. Aging (Albany NY) 2022;14:6936-56.
25. Han S, Zhu W, Yang W, et al. A Prognostic Signature Constructed by CTHRC1 and LRFN4 in Stomach Adenocarcinoma. Front Genet 2021;12:646818.
26. Jin H, Yu Z, Tian T, et al. Integrative Genomic and Transcriptomic Analysis of Primary Malignant Gliomas Revealed Different Patterns Between Grades and Somatic Mutations Related to Glioblastoma Prognosis. Front Mol Biosci 2022;9:873042.
27. Yan G, An Y, Xu B, et al. Potential Impact of ALKBH5 and YTHDF1 on Tumor Immunity in Colon Adenocarcinoma. Front Oncol 2021;11:670490.
28. Cui S, Feng J, Tang X, et al. The prognostic value of tumor mutation burden (TMB) and its relationship with immune infiltration in breast cancer patients. Eur J Med Res 2023;28:90.
29. Jiang Y, Yan Q, Liu CX, et al. Insights into potential mechanisms of asthma patients with COVID-19: A study based on the gene expression profiling of bronchoalveolar lavage fluid. Comput Biol Med 2022;146:105601.
30. Yang Y, Qu A, Wu Q, et al. Prognostic value of a hypoxia-related microRNA signature in patients with colorectal cancer. Aging (Albany NY) 2020;12:35-52.
31. Yu P, Tong L, Song Y, et al. Systematic profiling of invasion-related gene signature predicts prognostic features of lung adenocarcinoma. J Cell Mol Med 2021. [Epub ahead of print]. doi: 10.1111/jcmm.16619.
32. Yu H, Wang C, Ke S, et al. Identification of CFHR4 as a Potential Prognosis Biomarker Associated With Immune Infiltrates in Hepatocellular Carcinoma. Front Immunol 2022;13:892750.

33. Ding H, Shi L, Chen Z, et al. Construction and evaluation of a prognostic risk model of tumor metastasis-related genes in patients with non-small cell lung cancer. BMC Med Genomics 2022;15:187.
34. Obuchowski NA, Bullen JA. Receiver operating characteristic (ROC) curves: review of methods with applications in diagnostic medicine. Phys Med Biol 2018;63:07TR01.
35. Siegel RL, Miller KD, Fuchs HE, et al. Cancer statistics, 2022. CA Cancer J Clin 2022;72:7-33.
36. Chen Y, Jin L, Jiang Z, et al. Identifying and Validating Potential Biomarkers of Early Stage Lung Adenocarcinoma Diagnosis and Prognosis. Front Oncol 2021;11:644426.
37. Enfield KSS, Marshall EA, Anderson C, et al. Epithelial tumor suppressor ELF3 is a lineage-specific amplified oncogene in lung adenocarcinoma. Nat Commun 2019;10:5438.
38. Taya M, Garcia-Hernandez ML, Rangel-Moreno J, et al. Neutrophil elastase from myeloid cells promotes TSC2-null tumor growth. Endocr Relat Cancer 2020;27:261-74.
39. Chen X, Leahy D, Van Haeften J, et al. A Versatile and Robust Serine Protease Inhibitor Scaffold from Actinia tenebrosa. Mar Drugs 2019;17:701.
40. Na K, Hernandez-Prera JC, Lim JY, et al. Characterization of novel genetic alterations in salivary gland secretory carcinoma. Mod Pathol 2020;33:541-50.
41. Wolthers BO, Frandsen TL, Patel CJ, et al. Trypsin-encoding PRSS1-PRSS2 variations influence the risk of asparaginase-associated pancreatitis in children with acute lymphoblastic leukemia: a Ponte di Legno toxicity working group report. Haematologica 2019;104:556-63.
42. Rolland-Fourcade C, Denadai-Souza A, Cirillo C, et al. Epithelial expression and function of trypsin-3 in irritable bowel syndrome. Gut 2017;66:1767-78.

Cite this article as: Nie L, Zhang X, Wu J. PRSS3 is a potential prognostic biomarker for lung adenocarcinoma. Transl Cancer Res 2025;14(2):1124-1140. doi: 10.21037/tcr-24-1556